

1 This is a non-peer reviewed preprint that has been submitted to *Geochemical Journal*;
2 future versions may have different content.

3 **Title: Petrographic characteristics in the pumice clast deposited along the Gulf of**
4 **Thailand, drifted from Fukutoku-Oka-no-Ba**

5 Kenta Yoshida^{1*}, Yoshihiko Tamura¹, Tomoki Sato¹, Chalermrat Sangmanee²,

6 Ratchanee Puttapreecha², Shigeaki Ono¹

7
8 1 Research Institute for Marine Geodynamics, Japan Agency for Marine-Earth Science
9 and Technology (JAMSTEC). 2-15 Natsushima-cho, Yokosuka, 237-0061 Japan

10 2 Moo 3, Rattaprasasanabhakti Building, 5-9th Floor, Chaeng Watthana Road, Thung
11 Song Hong, Khet Lak Si, Bangkok, 10210 Thailand

12 **corresponding author, Kenta Yoshida, yoshida_ken@jamstec.go.jp, +81-46-867-**

13 **9782**

14 **Keywords:** pumice rafts; Fukutoku-Oka-no-Ba; Izu-Ogasawara arc; Gulf of Thailand,
15 South China Sea

16

17

18 **Abstract**

19 The 2021 eruption of Fukutoku-Oka-no-Ba (FOB) in the northwest Pacific on 13
20 August 2021 produced a large volume of pumice that drifted westward for ~1300 km to
21 the Nansei Islands, Japan, and some extent. In February 2022, pumice with similar
22 characteristics to the FOB pumice was deposited along along the Gulf of Thailand. The
23 pumice clasts deposited in Songkhla Province, Thailand, were <4 cm in length and
24 rounded. Most of the clasts consisted of clinopyroxene, plagioclase (andesine), and
25 olivine phenocrysts in a vesiculated grey groundmass, with black-coloured spots
26 exhibiting signatures of a basaltic magma. The whole-rock compositions of the pumice
27 are trachytic, with 61 mass% SiO₂ and 9 mass% total alkali (Na₂O + K₂O). The overall
28 characteristics in the pumice from Thailand are similar to those in FOB pumice. These
29 pumice in Thailand were from the 2021 FOB eruption, and drifted >2800 km south-
30 westward across the South China Sea.

31

32 **Keywords**

33 pumice rafts; Fukutoku-Oka-no-Ba; Izu-Ogasawara arc; Gulf of Thailand, South China

34 Sea

35

36 **Introduction**

37 Fukutoku-Oka-no-Ba (FOB) is a submarine volcano in the NW Pacific located at 24°

38 $17.1' \text{ N}/141^{\circ} 28.9' \text{ E}$, ~5 km northeast of Minami-Iōtō Island and ~1300 km south of

39 mainland Japan (Fig. 1a). The 2021 eruption occurred on the early morning of 13

40 August (Japan Standard Time) and produced a large amount of pumice that formed rafts

41 drifting to the west by the Kuroshio Counter-current, and drifting to many places in

42 Japan, Taiwan, and Philippines until December (Yoshida et al., 2022).

43 On 9 February 2022, a considerable amount of pumice was deposited on the beaches of

44 Songkhla province in southern Thailand and subsequently at Chumphon and Rayong

45 provinces in the north of the Gulf of Thailand (Fig. 1a, b). This pumice strongly

46 resembles the 2021 FOB pumice collected in Japan. The westward drifting of the FOB

47 pumice was also observed in 1986 eruption at ~200 km off the coast of Vietnam (16°

48 $28.2' \text{ N}, 110^{\circ} 24' \text{ E}$) on 28 August 1986 (Fig. 1a; Smithsonian Institution, 1986).

49 This paper aims at briefly describing the petrographic and geochemical characteristics

50 of the pumice collected in Thailand, comparing them with other FOB pumice collected
51 in Japan, and documenting the pumice raft dispersal.

52

53 **Methods**

54 Whole-rock compositions of representative pumice clasts were determined by X-ray
55 fluorescence (XRF) spectrometry (Rigaku ZSX Primus II) at the Japan Agency for
56 Marine-Earth Science and Technology (JAMSTEC), Yokosuka, Japan. Mineral and
57 glass compositions were determined using a field emission gun electron microprobe
58 (EMP) analyzer with five wavelength-dispersive X-ray detectors (JEOL, JXA-8500F) at
59 JAMSTEC. Details of the analytical procedure followed Yoshida et al. (2022).

60

61 **Petrography and Mineralogy**

62 The pumice clasts investigated in this study were collected from Thung Yai ($7^{\circ} 9.8'$
63 N, $100^{\circ} 35.9'$ E) and Samila ($7^{\circ} 12.6'$ N, $100^{\circ} 37.4'$ E) beaches in Songkhla
64 Province, Thailand, on 10 February 2022. The clasts are rounded compared to those
65 collected in the Nansei Islands and are <4 cm in length. Most clasts are monotonously

66 grey in color, although one clast is a mixture of black and grey parts (Fig. 1c). Goose
67 barnacles of <2 cm are often found on the clasts (Fig. 1c). The whole-rock compositions
68 of the representative grey pumice clasts from the two localities are listed in Table S1.
69 The pumice clasts consist of plagioclase (Pl), clinopyroxene (Cpx), and olivine (Ol)
70 phenocrysts in a vesiculated groundmass of volcanic glass, with a small amount of
71 apatite and opaque minerals (Fig. 2a). In addition, poorly vesiculated black enclaves
72 were identified (Fig. 2b). Representative mineral and glass compositions are listed in
73 Tables S1 and S2, respectively.

74 The whole-rock compositions yield SiO₂ contents of 61.6 and 61.8 mass% and total
75 alkali (K₂O + Na₂O) contents of 9.2 and 9.1 mass%, respectively, on an anhydrous
76 basis. These are almost identical to the FOB trachyte samples from the 2021 and earlier
77 eruptions (Fig. 2c). EMP analyses of the vesiculated glass in the grey groundmass yield
78 higher SiO₂ (65-66 mass%) and total alkali (10-10.6 mass%), while the interstice of the
79 type-1 black enclaves yield slightly lower SiO₂ (~64 mass%) and higher FeO* (~4.4
80 mass%).

81 Plagioclase in the groundmass has X_{An} (=Ca/[Ca+Na+K]) values of 0.41 and 0.32 in the

82 core and rim, respectively. Glass associated with or included as melt inclusions in
83 coarse-grained plagioclase is brown and yields a similar composition to the colourless
84 groundmass glass (Table S1). Clinopyroxene in the groundmass is augite, with Mg#
85 ($=\text{Mg}/[\text{Mg}+\text{Fe}] \times 100$) of 76. Olivine in the groundmass yields Mg# of 65. High-Mg
86 (Mg# ~90) olivine crystals occur in the mixed black and grey pumice clast (SM-01) and
87 are associated with brown glass (Table S2).

88 The black enclaves consist of clinopyroxene and plagioclase phenocrysts in a poorly
89 vesiculated groundmass with abundant clinopyroxene, plagioclase, and magnetite
90 microlites of $<100 \mu\text{m}$ in length (Fig. 2b). Olivine microlites are possibly also present,
91 although individual analyses could not be carried out due to their small size. Plagioclase
92 phenocrysts in the black enclave have X_{An} values of 0.95, and contain basaltic melt
93 inclusions with SiO_2 contents of 47 mass%. The interstitial glass in the black enclave
94 yields trachytic composition (Table S1). These characteristics are the similar to those of
95 the type-1 black enclave found in the grey FOB pumice (Yoshida et al., 2022)

96

97 **Implications**

98 The petrographic and geochemical characteristics of the pumice clasts in the raft that
99 arrived in Thailand are similar to those of the FOB pumice observed on the coast of
100 Japan (Yoshida et al., 2022). In particular, the poorly vesiculated black enclaves in the
101 pumice from Thailand are similar to the type-1 black enclaves reported in the FOB
102 pumice. These observations suggest that the pumice raft from the 2021 FOB eruption
103 drifted another ~2800 km from Luzon Strait to Thailand in ~ 80 days (Fig. 1a). The
104 South China Sea (SCS) lies in the monsoon regime, and strong northeast winds prevail
105 over the region during winter (~9 m/s on average; Hu et al., 2000), which enabled the
106 pumice raft to be transported over the SCS.

107 The areal extent of the raft dispersal would provide a better understanding of pumice
108 rafting and related disaster prevention. Records of the locations and arrival times of
109 pumice rafts are crucial for disaster prevention in the Circum-Pacific belt. An
110 international pumice monitoring network might be required for future large eruptions.

111 **Acknowledgements**

112 This work was partly supported by JSPS KAKENHI JP19K14825 for KY.

113 **References**

114 Bryan, S.E., Cook, A.G., Evans, J.P., Hebden, K., Hurrey, L., Colls, P., Jell, J.S.,
115 Weatherly, D., and Finn, J. (2012) Rapid, long-distance dispersal by pumice rafting.
116 *Plos one* 7, e40583.

117 Hu, J., Kawamura, H., Hong, H., Qi, Y. (2000) A review on the currents in the South
118 China Sea: Seasonal circulation, South China Sea warm current and Kuroshio
119 Intrusion. *J. of Oceanograph.* 56, 607-624.

120 Smithsonian Institution (1986) Pumice from unknown source clogs ship's intakes.
121 *Scientific Event Alert Network (SEAN) Bulletin* 11:12.

122 Yoshida, K., Tamura, Y., Sato, T., Hanyu, T., Usui, Y., Chang, Q., & Ono, S. (2022)
123 Variety of the drift pumice clasts from the 2021 Fukutoku-Oka-no-Ba eruption,
124 Japan. *Isl. Arc* 31, e12441.

125

126 **Figure legends**

127 **Figure 1** (a) Summary of the arrival dates of drifting pumice modified after Yoshida et
128 al. (2022). Yellow star indicates the raft recognition in 1986 (Smithsonian Institution,
129 1986). (b) Dark grey pumice deposit at Thung Yai beach in Songkhla Province,

130 Thailand, on 10 February 2022. (c) Grey pumice clasts collected on Samila beach in
131 Songkhla Province, Thailand, with black spots and often with attached goose barnacles.
132 One clast contained a black pumice band.

133

134 **Figure 2** (a) Photomicrograph of a pumice clast collected from Thung Yai beach
135 (sample TY-1) in Songkhla Province. Plagioclase (Pl), clinopyroxene (Cpx), and olivine
136 (Ol) phenocrysts were observed. The glass adhering to, and as melt inclusions in, Pl
137 phenocrysts is brown, whereas the groundmass glass is colourless. “Vac” indicates a
138 vesicle. (b) Backscattered electron image of the black enclave in TY-1. Anorthite-rich
139 Pl and diopsidic Cpx with an augitic rim occur in the poorly vesiculated groundmass of
140 the black enclave that contained ubiquitous magnetite. (c) Total alkali ($\text{Na}_2\text{O} + \text{K}_2\text{O}$)
141 versus SiO_2 diagram for the classification of volcanic rocks, showing the whole-rock
142 and glass compositions of pumice clasts from Thailand. Previously reported data for
143 pumice rafts from the 2021 eruption of FOB are also shown (Yoshida et al., 2022).

144

145 **Table S1.** Whole rock and groundmass glass compositions of the pumice.

146 Footnote: FeO*, total iron as FeO. n.a., not analysed.

147

148 **Table S2.** Representative mineral compositions.

149 Footnote: FeO*, total iron as FeO. $\text{Fe}^{3+}/\text{Fe}^{2+}$ was determined as follows: total cation =4

150 (clinopyroxene), $(\text{Fe}^{2+} + \text{Mg} + \text{Mn}) = 1$ (magnetite).

151

Figure 1

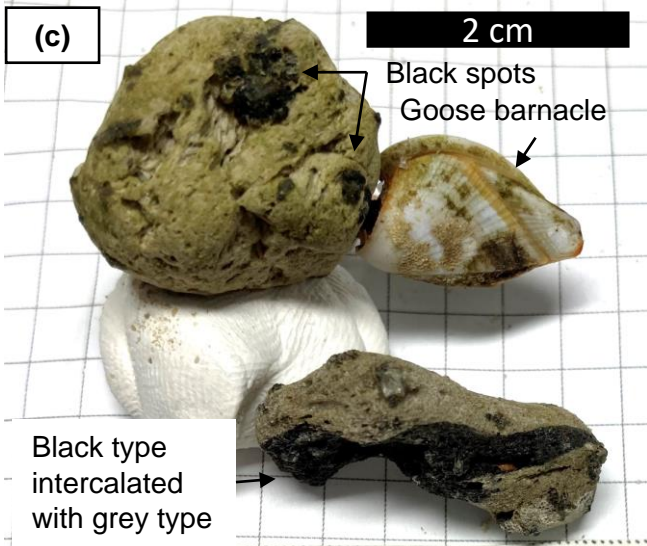
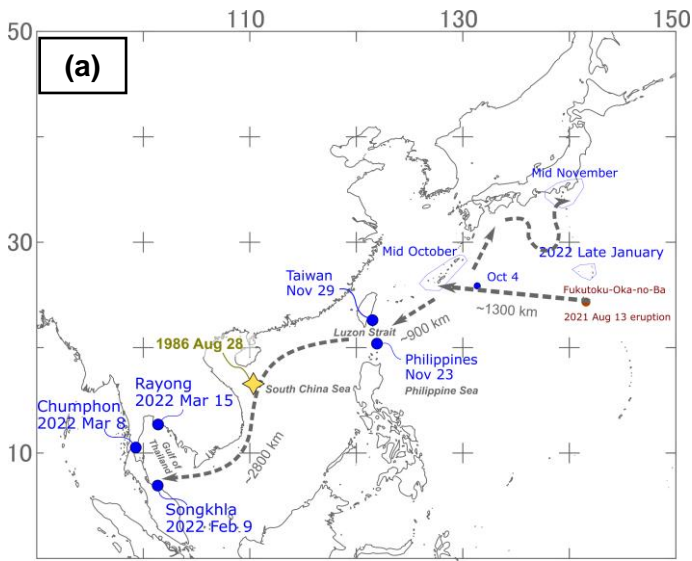


Figure 2

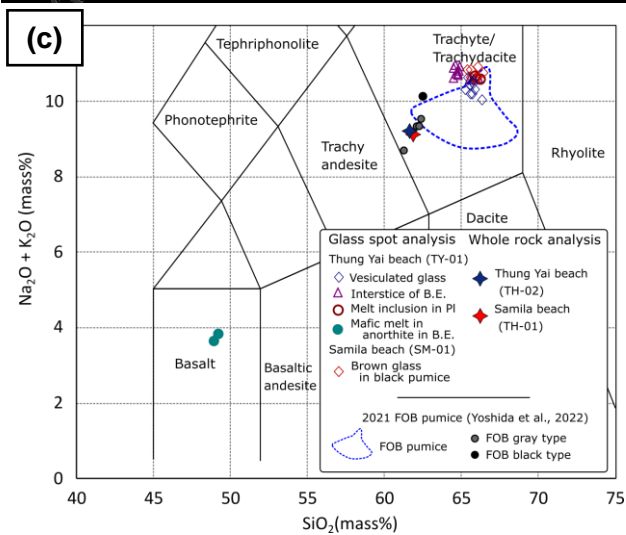
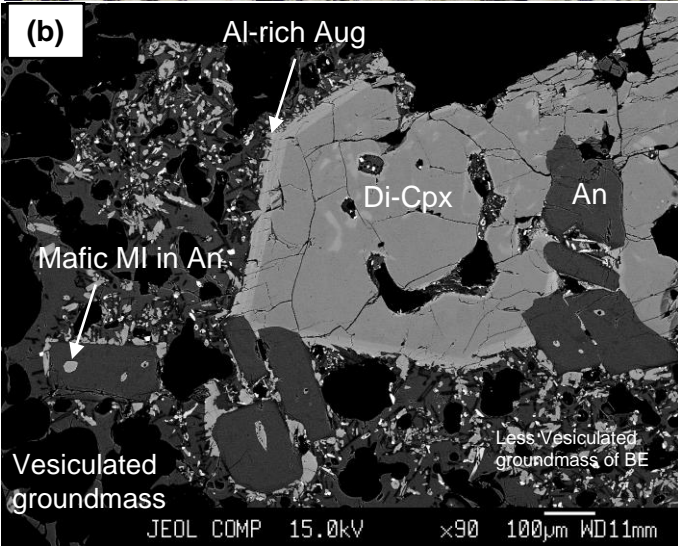
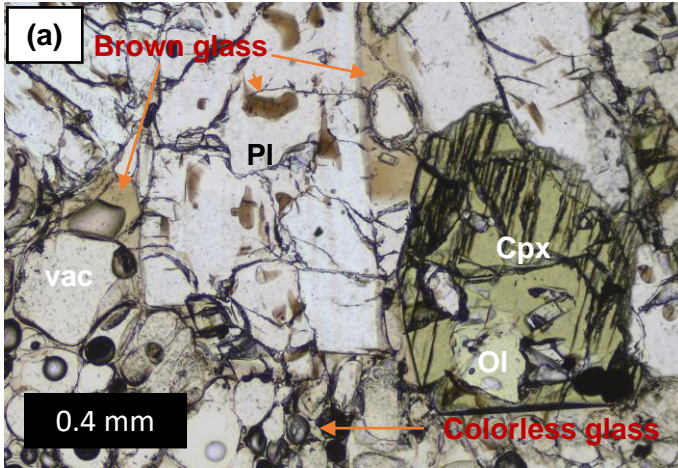


Table S1

Sample No.	XRF whole rock analysis		EMP spot analysis				SM-01
	TH-01	TH-02	TY-01				
locality	Samila beach	Thung Yai beach	Thung Yai beach		Black enclave in gray pumice		Samila beach
occurrence			Gray pumice		Black enclave in gray pumice		Black pumice
			groundmass	melt inclusion in plagioclase	interstice in black enclaves	melt inclusion in anorthite	brown glass
n=			10	10	10	2	8
SiO ₂	60.748	60.497	65.07	64.94	64.29	46.95	65.35
TiO ₂	0.567	0.584	0.51	0.48	0.42	0.86	0.48
Al ₂ O ₃	15.971	16.031	16.22	16.16	16.37	11.33	16.17
Cr ₂ O ₃	n.a.	n.a.	0.00	0.01	0.03	0.01	0.03
FeO*	5.447	5.589	3.95	3.41	4.41	13.29	3.71
MnO	0.17	0.171	0.17	0.12	0.14	0.22	0.11
MgO	2.51	2.516	1.08	0.75	0.99	8.52	0.82
CaO	4.189	4.094	1.79	1.69	1.70	10.97	1.91
Na ₂ O	4.53	4.602	5.02	5.15	5.23	2.23	5.29
K ₂ O	4.42	4.435	5.22	5.24	5.42	1.35	5.31
P ₂ O ₅	0.23	0.232	0.16	0.16	0.24	0.16	0.19
F	n.a.	n.a.	0.12	0.12	0.12	0.27	0.09
Cl	n.a.	n.a.	0.29	0.32	0.36	0.12	0.32
total	98.782	98.751	99.60	98.56	99.72	96.27	99.79
LOI	0.64	0.64					

Table S2

Sample	TY-01											SM-01
occurenc	Gray pumice, phenocryst					Black enclave, phenocryst			Black enclave, microlite			with brown glass
	Pl, core	Pl, rim	Cpx	Ol	Mag	Pl	Cpx, core	Cpx, rim	Pl	Cpx	Mag	Ol
SiO2	57.88	59.88	53.13	37.56	0.12	44.40	50.35	46.268	56.851	44.774	0.268	41.05
TiO2	0.02	0.03	0.29	0.00	10.47	0.00	0.38	0.888	0.139	0.977	7.527	0.01
Al2O3	25.86	24.16	1.55	0.02	2.98	34.40	4.46	8.605	26.035	10.234	3.673	0.02
Cr2O3	0.00	0.04	0.05	0.00	0.01	0.02	0.00	0	0.01	0.02	0.069	0.04
FeO*	0.57	0.47	9.32	30.84	77.97	0.92	6.38	9.272	0.948	10.653	77.843	9.87
MnO	0.03	0.08	0.75	1.87	1.07	0.03	0.20	0.095	0.012	0.146	0.539	0.19
MgO	0.00	0.05	15.26	31.91	2.94	0.10	15.22	12.578	0.121	12.017	2.805	49.10
CaO	8.67	6.72	19.85	0.41	0.06	19.13	22.92	22.064	9.437	20.917	0.115	0.26
Na2O	6.36	7.13	0.40	0.03	0.00	0.57	0.14	0.207	5.602	0.263	0	0.00
K2O	0.79	1.10	0.02	0.00	0.02	0.04	0.01	0.017	0.88	0.042	0.08	0.01
total	100.19	99.66	100.63	102.64	95.62	99.62	100.06	99.99	100.04	100.04	92.92	100.53
O=	8	8	6	4	3	8	6	6	8	6	3	4
Si	2.60	2.69	1.96	1.00	0.00	2.07	1.85	1.72	2.57	1.66	0.01	1.00
Ti	0.00	0.00	0.01	0.00	0.22	0.00	0.01	0.02	0.00	0.03	0.16	0.00
Al	1.37	1.28	0.07	0.00	0.10	1.89	0.19	0.38	1.39	0.45	0.12	0.00
Cr	0.00	0.00	0.00	0.00	0.00	0.00	0.00	0.00	0.00	0.00	0.00	0.00
Fe3+			0.03		0.94		0.10	0.14		0.20	0.98	
Fe2+	0.02	0.02	0.26	0.69	0.85	0.04	0.10	0.14	0.04	0.13	0.87	0.20
Mn	0.00	0.00	0.02	0.04	0.02	0.00	0.01	0.00	0.00	0.00	0.01	0.00
Mg	0.00	0.00	0.84	1.26	0.12	0.01	0.83	0.70	0.01	0.67	0.12	1.78
Ca	0.42	0.32	0.78	0.01	0.00	0.95	0.90	0.88	0.46	0.83	0.00	0.01
Na	0.55	0.62	0.03	0.00	0.00	0.05	0.01	0.01	0.49	0.02	0.00	0.00
K	0.05	0.06	0.00	0.00	0.00	0.00	0.00	0.00	0.05	0.00	0.00	0.00
XAn	0.41	0.32				0.95			0.46			
XAb	0.54	0.62				0.05			0.49			
Xor	0.04	0.06				0.00			0.05			
Mg#			76	65			89	83		83		